Simultaneous Optical and Electrical Recording of Single Gramicidin Channels

V. Borisenko,* T. Lougheed,* J. Hesse,[†] E. Füreder-Kitzmüller,[†] N. Fertig,[‡] J. C. Behrends,[‡] G. A. Woolley,* and G. J. Schütz[†]

*Department of Chemistry, University of Toronto, Toronto M5S 3H6, Canada; [†]Institute for Biophysics, Johannes Kepler Universität, A-4040 Linz, Austria; and [‡]Center for Nanoscience, Ludwig Maximilians Universität, 80539 Munich, Germany

ABSTRACT   We report here an approach for simultaneous fluorescence imaging and electrical recording of single ion channels in planar bilayer membranes. As a test case, fluorescently labeled (Cy3 and Cy5) gramicidin derivatives were imaged at the single-molecule level using far-field illumination and cooled CCD camera detection. Gramicidin monomers were observed to diffuse in the plane of the membrane with a diffusion coefficient of 3.3×10^{-8} cm^{2}s^{-1}. Simultaneous electrical recording detected gramicidin homodimer (Cy3/Cy3, Cy5/Cy5) and heterodimer (Cy3/Cy5) channels. Heterodimer formation was observed optically by the appearance of a fluorescence resonance energy transfer (FRET) signal (irradiation of Cy3, detection of Cy5). The number of FRET signals was significantly smaller than the number of Cy3 signals (Cy3 monomers plus Cy3 homodimers) as expected. The number of FRET signals increased with increasing channel activity. In numerous cases the appearance of a FRET signal was observed to correlate with a channel opening event detected electrically. The heterodimers also diffused in the plane of the membrane with a diffusion coefficient of 3.0×10^{-8} cm^{2}s^{-1}. These experiments demonstrate the feasibility of simultaneous optical and electrical detection of structural changes in single ion channels as well as suggesting strategies for improving the reliability of such measurements.

INTRODUCTION

Ion channel gating underlies the electrical behavior of cells and tissues. The functional behavior of ion channels can be studied at single-molecule resolution using the patch-clamp technique (Sakmann and Neher, 1984) that permits electrical detection of ion flux through individual channels. This technique has provided a wealth of functional detail on many channels, but in most cases connecting this information to the structures and dynamics of channel proteins has proved difficult (e.g., Sigworth, 1994; Maduke et al., 2000). Recently, fluorescence resonance energy transfer (FRET) methods have been employed to measure structural changes in ensembles of ion channels that can be triggered by a change in transmembrane voltage (Cha et al., 1999; Glauner et al., 1999). Data from such measurements can be used to construct molecule models of the voltage gating process.

Recent advances in single molecule fluorescence methods have made possible the observation of fluorescently labeled ion channels under near native conditions (Schütz et al., 2000a; Harms et al., 2001). Such experiments have the potential to provide structural information on single molecules at the same time that their function is being observed via electrical recording techniques (MacDonald and Wraight, 1995; Helluin et al., 1997; Ishii and Yanagida, 2000; Ide and Yanagida, 1999). As well as permitting the study of channels whose gating transitions cannot be synchronized, this approach might uncover aspects of channel function (e.g., allosteric interactions among channel

subunits) that are necessarily obscured in an ensemble measurement.

The single dye tracing approach (Schmidt et al., 1996; Schütz et al., 2000b) seems particularly amenable for studying ion channels under conditions typical for electrophysiological measurements. The method can be used to image relatively large ($\sim$400 μm^2) bilayer membranes and can achieve single molecule sensitivity with a time resolution of $\sim$5 ms. The technique has been used to image the diffusion of dye-labeled lipid molecules in unsupported membranes painted across an aperture in a Teflon film (Sonnleitner et al., 1999)—the same type of membrane typically used to study reconstituted ion channels (Anzai et al., 2001). To examine the feasibility of combining optical and electrical detection of channels using this technique, we decided to examine the behavior of fluorescently labeled gramicidin peptides as a test case.

The small peptide ion channel gramicidin A (gA) has served as a model system for understanding fundamental aspects of ion channels for more than 30 years. It was the first channel for which a primary structure was determined (Sarges and Witkop, 1965); it was the first defined substance for which single-channel currents were observed via electrical recording (Hladky and Haydon, 1970), and it was the first channel for which the three-dimensional structure of the conducting form was determined (Arseniev et al., 1985; Ketchem et al., 1993). Moreover, simultaneous optical and electrical measurements—in a multichannel format—were made by Veatch and Stryer 25 years ago (Veatch et al., 1975) in a landmark work that helped to establish the basic mechanism of gA channel formation. The gramicidin gating event (channel opening) is widely believed to be the dimerization of peptides in the membrane (e.g.,

Goulian et al., 1998; Woolley and Wallace, 1992). The conducting form of the gA channel is an N-terminus to N-terminus dimer that is a $\beta^{6.3}$ helix $\sim$28 Å long and 4 Å in diameter (Koeppe and Anderson, 1996) (Fig. 1). The pore is lined by backbone amide groups and permits the trans-membrane flux of small monovalent cations, protons, and water. At 25°C the average lifetime of a dimer is on the order of 1 s.

Under the conditions of single-channel electrical recording measurements, gramicidin peptides occur predominantly as monomers in membranes. The equilibrium between monomers and dimers depends on the membrane type and the particular derivative of gramicidin (Koeppe et al., 1985; Veatch et al., 1975; Elliott et al., 1983; Bamberg and Lauger, 1973). The membranes commonly used for
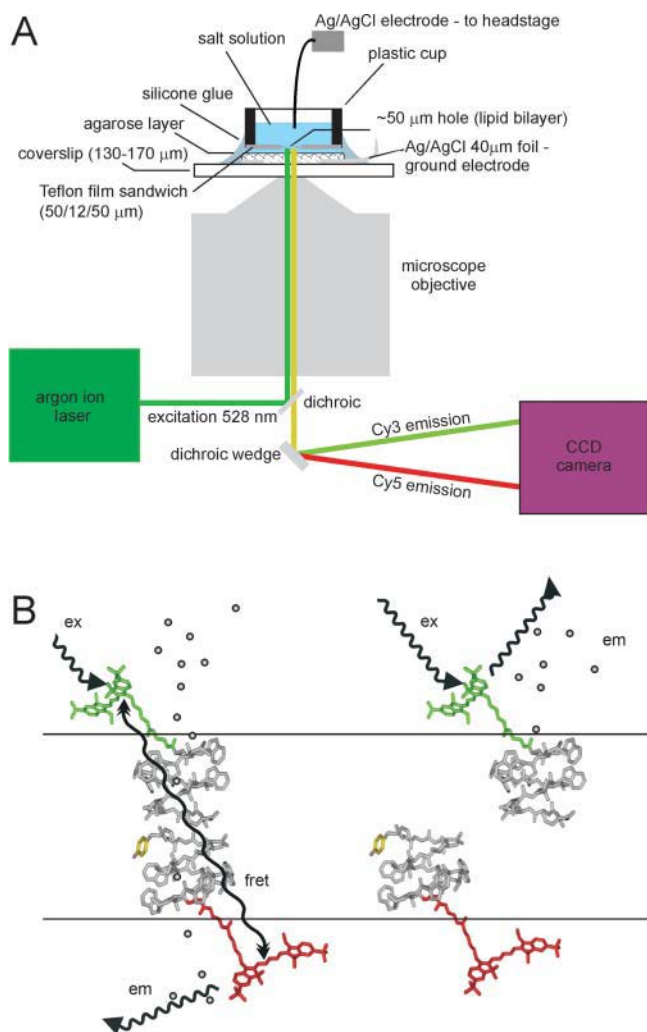

FIGURE 1 (A) Schematic diagram of the experimental arrangement for combined optical and electrical detection of single channels. (B) Schematic diagram showing channel formation by gA-Cy3 donor and *p*F-Phe-gA-Cy5 acceptor peptides. Peptide monomers diffuse in the plane of the bilayer (*shown as two parallel lines*). Dimerization results in a pathway for ions (*small circles*) across the membrane and also brings the Cy3 and Cy5 dyes into close proximity ($\sim$50 Å) so that FRET occurs.

gramicidin single-channel measurements are made from diphytanoyl-phosphatidylcholine dissolved in *n*-decane. Although, to our knowledge, a value of the dimerization constant (K_A) has not been measured for these membranes directly, an estimate of 10^{14} cm²/mol can be made based on data from closely related membranes (Veatch et al., 1975). For single-channel experiments, gramicidin is added to lipid at a mole ratio of $\sim$1:10^7, to give a total surface density of $\sim$10^{-16} mol/cm² (assuming 0.63 nm²/lipid (Selig, 1981)). With $K_A = 10^{14}$ cm²/mol, this gives an average of $\sim$100 monomers for each dimer. Previous measurements of lipid diffusion in bilayers using single dye tracing methods have shown that fluorophore/lipid ratios of 1/10^7 are suitable to permit single molecule resolution (i.e., overlap of signals from different labeled molecules is not too severe) (Schmidt et al., 1996). However, inasmuch as the fluorescence signal from monomers is expected to greatly outweigh that from dimers, we decided to employ fluorescence energy transfer to be able to detect dimers in the presence of a relatively large number of monomers. The power of single-pair FRET for detecting structural changes in biological systems has been recently reviewed (Ha, 2001).

EXPERIMENTAL

Synthesis of fluorescently labeled peptides

Synthesis of desformyl gramicidin D

Methanol (15 mL)(HPLC grade) was placed in a 50-mL round-bottom flask and cooled in an ice bath to 0°C. Freshly distilled acetyl chloride (3 mL) (Aldrich) was added dropwise to the cold methanol. The reaction vessel was removed from the ice bath, allowed to reach room temperature, and left for a further 30 min. The flask was again cooled to 0°C and a solution of 290 mg gramicidin D (Sigma) dissolved in 1.0 mL of methanol was added dropwise. After complete addition of the gramicidin solution, the flask was again removed from the ice bath and left for a further 3 h at room temperature. Thin layer chromatography of the reaction mixture showed nearly complete conversion to the desformyl product after 3 h. The solvents were removed by rotary evaporation followed by drying under high vacuum to yield 260 mg of a fine white powder (90% yield). The product was verified by matrix-assisted laser desorption/ionization mass spectrometry (MALDI-MS). This desformyl gramicidin was used directly in the next step without further purification. Desformyl-gramicidin = $C_{98}H_{140}N_{20}O_{16}$ [MH]$^+$ calculated = 1854.3 observed = 1854.1; thin layer chromatography (TLC) (C:M:W = 65:35:4): gramicidin R_f = 0.75, desformyl-gramicidin R_f = 0.64.

Synthesis of des(formylvalyl)gramicidin D

The procedure to prepare des(formylvalyl)gramicidin D was identical to that described by Weiss and Koeppe, 2nd (1985). Briefly, 250 mg (0.14mmol) of desformyl-gramicidin were dissolved in 10 mL of pyridine and 0.5 mL of dry, freshly distilled triethylamine (Aldrich) under an argon atmosphere. Phenylisothiocyanate (75 μL)(0.7mmol)(Aldrich) was added, and the solution stirred for 1.5 h at 40°C under argon. Aniline (100 μL) was added after 1 h to quench excess phenylisothiocyanate. After an additional 10 min at 40°, the solvents were evaporated under high vacuum. Once all solvents had been removed, the product was dissolved in 5.0 mL of methanol, and the PTH-valine was cleaved by addition of anhydrous 4 N HCl in dioxane (Aldrich). After 1 h at room temperature, the sample was again evaporated to

dryness. The product was purified by gel filtration using Sephadex LH-20 (2.0 cm $\times$ 70 cm gravity column) and verified by electrospray-MS. Des(formylvalyl)gramicidin = $C_{93}H_{131}N_{19}O_{15}$ [MH]$^+$ calculated = 1755.2 observed = 1754.7; TLC (C:M:W: = 65:25:4): R_f = 0.64 taken at the center of a broad spot. The spot stained purple with DMAB and orange with ninhydrin.

Formylation of pF-phenylalanine

The procedure for the preparation of the N-formylamino acid was essentially the same as that described by Greathouse et al. (1999). Briefly, 100 mg (0.5 mmol) of pF-phenylalanine (Bachem) was dissolved in 1.2 mL (32 mmol) of formic acid (96%). While stirring in an ice bath under nitrogen, 0.4 mL (4 mmol) of acetic anhydride was added dropwise. This solution was allowed to stir for a period of at least 24 h. The solvents were evaporated and the resulting product dissolved in methanol. The formylamino acid was precipitated out of solution by addition of excess water and vacuum filtered. The product was verified by electrospray-MS and used directly in the next step without further purification. Formyl-pF-phenylalanine = $C_{10}H_{10}NO_3F$ [MH]$^+$ calculated = 211.2 observed = 210.9. TLC (C:M:W: = 65:25:4): pF-phenylalanine R_f = 0.25, formyl-pF-phenylalanine R_f = 0.45 (taken at the center of a broad spot). The starting material showed intense staining with ninhydrin whereas the formylated product did not.

Coupling of formyl-pF-phenylalanine with des(formylvalyl)gramicidin

The procedure for the preparation of formyl-pF-phenylalanine des(formyl-valyl)gramicidin followed that of Weiss and Koeppe, 2nd (Weiss and Koeppe, 1985). Des(formylvalyl) gramicidin (54 mg)(31 μmol) was dissolved in 1.0 mL of dry dimethylformamide (DMF). The flask was placed on ice and cooled to 0°C. Formyl-pF-phenylalanine (18 mg) (84 μmol) was dissolved in 0.5 mL of dry DMF and added to the reaction vessel via syringe; ~10 μL (49 μmol) of dry, freshly distilled diisopropylethylamine (Aldrich) was also added to the reaction. Finally 8.5 μL (49 μmol) of diphenylphosphorylazide (DPPA) (Fluka) was added via syringe to the cold, stirring solution. After 1.25 h at 0°C, the solvents were removed under high vacuum and the crude mixture resuspended in methanol. The product was precipitated by adding excess water and then lyophilized to give a fine white powder. The product was purified by gel filtration using Sephadex LH-20 (2.0 cm $\times$ 70 cm gravity column), and the fractions containing typical gramicidin-type absorbance at 280 nm collected, whereas the fractions containing only absorbance representative of the free, uncoupled amino acid (~260 nm) were discarded. The product was verified by MALDI-MS. Formyl-pF-Phe-des(formylvalyl) gramicidin A = $C_{103}H_{139}N_{20}O_{17}F$ calculated = 1948.4 observed = 1947.8; TLC (C:M:W: = 65:25:4): Des(formylvalyl) gramicidin R_f = 0.64, formyl-pF-Phe-des(formylvalyl) gramicidin R_f = 0.75. The coupled product stained purple with DMAB and showed no stain with ninhydrin.

Synthesis of formyl-pF-phenylalanine-des(formylvalyl) gramicidin-ethylenediamine (pF-Phe-gD-EDA)

pF-Phe-gramicidin D (20 mg)(10.3 μmol) was dissolved in 1.0 mL of dry tetrahydrofuran in a flame-dried round-bottom flask that had been thoroughly flushed with nitrogen and immersed in an ice bath. Fresh p-nitrophenyl chloroformate (28 mg)(140 μmol)(Aldrich) was dissolved in 1.0 mL of dry tetrahydrofuran and added to the gramicidin solution. Freshly distilled dry triethylamine (TEA) (50 μL) was then added to the stirring reaction mixture dropwise. The solution immediately became cloudy and remained white for the duration of the 1 h reaction. A TLC of the reaction at this point showed clear conversion to the carbonate ester derivative (R_f = 0.91) with no remaining unreacted pF-Phe-gramicidin D. After 1 h, 65 μL (970 μmol) of ethylenediamine (EDA) was added via syringe and left to stir

for an additional hour. The solvents were removed by rotary evaporation followed by high vacuum. The mixture was then resuspended in methanol and purified by gel filtration using Sephadex LH-20. Fractions were collected based on the characteristic gramicidin UV-Vis absorbance spectrum and by the lack of yellow color that would indicate the presence of p-nitrophenol. pF-Phe-gramicidin-EDA = $C_{106}H_{145}N_{22}O_{18}F$ calculated = 2034.42 observed = 2034.4; TLC (C:M:W: = 65:25:4): pF-Phe-gramicidin-EDA R_f = 0.65. The product showed intense staining with both DMAB and ninhydrin.

Before labeling the peptide with Cy5, HPLC purification was necessary. An isocratic separation (80% methanol, 20% water (containing 0.1% trifluoroacetic acid adjusted to a pH of 3 with TEA)) was performed (1 mL/min) using a Zorbax Rx-C8 column. The UV-Vis detector was set to 280 nm. The largest peak (6.4 min) corresponded to the gramicidin A derivative (of the A, B, C mixture) as verified by MALDI-MS. After each run the column was purged with 100% methanol for 5 min to remove any gramicidin derivatives retained.

Labeling of pF-Phe-gA-EDA with Cy5

pF-Phe-gA-EDA (0.6 mg)(0.3 μmol) was placed in a 5-mL, two-neck round-bottom flask. The residual methanol solvent was removed under a gentle stream of nitrogen then further dried under high vacuum. The flask was successively evacuated and filled with nitrogen several times to ensure a nitrogen environment. The dried peptide was then dissolved in 400 μL of dry DMF. One package (~0.3 mg) of commercial Cy5 monoreactive N-hydroxysuccinimide ester (Amersham) was dissolved in 100 μL of dry DMF and added to the stirring reaction via syringe. Dry TEA (100 μL) was then added to the reaction mixture dropwise. The reaction progress was monitored via TLC using 65:25:4 C:M:W as the solvent system. Free dye generally gives two spots on TLC corresponding to the amount of activated versus hydrolyzed succinimidyl ester. The intact ester has an R_f value of 0.38 (the hydrolyzed form has a lower R_f value). pF-Phe-gA-EDA has an R_f value of 0.65. The product spot had an intermediate R_f value of 0.58 and was also characteristically blue. If unlabeled peptide remained, as determined by staining the plate with DMAB, a second dye package was added in the same fashion as described above. The reaction was left to stir for 24 h after which the DMF was removed under high vacuum and the product resuspended in methanol. pF-Phe-gA-EDA-Cy5 = $C_{139}H_{182}N_{24}O_{25}S_2F$ calculated = 2672.21 observed = 2672.8; TLC (C:M:W 65:25:4) R_f = 0.51.

HPLC purification of pF-Phe-gA-EDA-Cy5

The conditions for HPLC purification were identical to those described earlier. Unfortunately, the product (pF-Phe-gA-EDA-Cy5) had a retention time of 6.4 min, which is identical to that of the starting material (pF-Phe-gA-EDA). Thus, to separate unreacted pF-Phe-gA-EDA starting material from the dye-labeled product, acetic anhydride was added to the crude product in excess. The goal was to acetylate the free amine of the EDA precursor to effect a change of the retention time. As expected, the peak at 6.4 min remained (with a diminished intensity) and a new peak with a longer retention time (10 min) appeared. MALDI-MS confirmed the first peak to be the Cy5 labeled product and the second to be the acetylated EDA product ([MH]$^+$ = 2671.32). Double HPLC purification of pF-Phe-gA-EDA-Cy5 resulted in channel records that were essentially free of pF-Phe-gA-EDA. (Note that in the text, pF-Phe-gA-EDA-Cy5 is referred to as pF-Phe-gA-Cy5 for simplicity. Similarly, gA-EDA-Cy3 is referred to as gA-Cy3.)

Synthesis of gA-EDA-Cy3

Gramicidin-EDA was prepared as described above for pF-Phe-gramicidin-EDA and HPLC purified to isolate the gramicidin A form. The procedure for preparing gA-EDA-Cy3 was essentially the same as that described for pF-Phe-gA-EDA-Cy5. Gramicidin-A-EDA (1 mg)(0.5 μmol) was dissolved in 100 μL of dry DMF ensuring a nitrogen environment as described above.

One package of commercial Cy3 (Amersham)(~0.3 mg) was dissolved in 100 μL of dry DMF and added to the reaction vessel dropwise. Dry, freshly distilled TEA (20 μL) was then added to the reaction vessel and was left to stir for several hours. The course to the reaction was monitored via TLC, again showing the appearance of a new spot with an intermediate R_f value between that of the free dye and the gA-EDA precursor. A second vial of dye was dissolved in 100 μL dry DMF, added dropwise and left to react for 24 h. After this time, the solvents were removed under high vacuum and the crude product resuspended in methanol. gA-EDA-Cy3 = $C_{133}H_{181}N_{24}O_{25}S_2$ calculated = 2580.14, observed = 2580.2; TLC (C:M:W 65:25:4) $R_f = 0.5$.

HPLC purification of gA-EDA-Cy3

As with the Cy5 derivative, excess acetic anhydride was added to react with the remaining unlabeled gramicidin-EDA to give better separation from the labeled product and thus increase the recovery of the labeled peptide. The procedure was identical to that described above. Double HPLC purification of gA-EDA-Cy3 resulted in channel records that were essentially free of gA-EDA.

Characterization of fluorescent gramicidin derivatives in lipid vesicles

Unilamellar lipid vesicles containing gramicidin derivatives were prepared as follows: an aliquot of dioleoyl-phosphatidylcholine (Avanti Polar Lipids)(2 mg, 2.54 μmol) dissolved in methanol was added to a 1.5-mL Eppendorf tube containing either a given number of moles (e.g.,1 nmol) of an individual fluorescent gramicidin derivative or a 1:1 mixture (e.g., 0.5 nmol each) of two fluorescent gramicidin derivatives (total methanol volume = 400 μL). Concentrations of fluorescent gramicidins were determined by UV-Vis absorbance measurements of stock solutions in methanol. Methanol was then removed under a gentle stream of dry nitrogen to form a thin lipid film, and the film was pumped under high vacuum for >2 h. The lipid/gramicidin film was resuspended in 400 μL of 400 mM KCl, 6.5 mM phosphate buffer, pH 7.0. Unilamellar vesicles containing fluorescent gramicidins were then formed by repeated extrusion (20 passes) of the lipid suspension through a polycarbonate membrane (Avanti Polar Lipids) with a pore diameter of 100 nm. Fluorescence measurements were made of vesicle solutions prepared from 1:1 mixtures of fluorescent gramicidins and compared to measurements of 1:1 mixtures of vesicle solutions prepared from pure fluorescent gramicidins. Final lipid concentrations and peptide concentrations are given in figure legends. Steady-state fluorescence measurements were made using a Perkin-Elmer LS50B spectrofluorimeter (equipped with a red-sensitive photomultiplier for Cy5 detection) and a 150-μL cuvette with 0.5-cm excitation and emission pathlengths. All measurements were made at room temperature (23 $\pm$ 2°C).

Single-channel electrical and optical measurements

Cell design

The cell design is shown in Fig. 1. A thin circular Teflon sandwich separated two aqueous phases situated below and above it. The sandwich had a diameter of 17 mm and consisted of three thin Teflon disks 50, 12, and 50 μm thick sealed together at high temperature. The two outside 50-μm disks had ~3-mm holes in the center. A small hole ~40–70 μm in diameter was made with a hot needle in the center of the 12-μm disk. The Teflon sandwich was then glued with silicone glue to a short (~6 mm) cylindrical plastic pipe having the same diameter as a Teflon disk to make the top chamber of the cell (*plastic cup*, Fig. 1).

A disk of chlorided silver foil (50-μm thick) ~17 mm in diameter with a ~10-mm hole in the center was placed on a glass coverslip. The disk was covered in a thin (<100 μm) layer of agarose and functioned as the Ag/AgCl

electrode. To create the bottom chamber, one to two drops of the buffer solution were placed on the coated glass coverslip. The top chamber was then pressed onto the glass coverslip and glued with silicone glue leaving a short silver foil tail coming out through the glue from the bottom chamber to allow electrical contact. After the silicone glue dried (~1 h), the buffer solution was added to the top cylinder chamber and another Ag/AgCl electrode was placed in it. Each cell was used once only, and before each experiment a fresh one was built. The cell was mounted horizontally in a copper box that had a drilled hole in the bottom to allow the microscope objective to contact the bottom side of the glass coverslip.

Electrical and optical recording

Peptides (~10 nM in methanol) were added to membranes formed from diphytanoyl-phosphatidylcholine/decane (50 mg/mL). In case of hybrid channel experiments, different peptides were added to the same cylindrical chamber of the cell. Lipid bilayers were formed across the 40–70-μm hole in the Teflon disk by painting a solution of lipid in decane from the top. Symmetrical buffered (5 mM BES) KCl (1 M) solutions were used. After a stable bilayer was formed with a desired single-channel activity, the copper box with the cell inside was carefully mounted on the optical stage of the microscope in such a way that the laser irradiated the cell from the bottom of the box. All measurements were made at room temperature.

Currents through lipid bilayers containing the gramicidin derivatives were measured and voltage was set using an Axopatch-1D patch-clamp amplifier (Axon Instruments). Data were digitized and then analyzed using either Synapse (Synergistic Research Systems) or Clampex (Axon Instruments) software. For histograms, single-channel events were recorded for a period of several hours for each set of experimental conditions. Mean lifetimes and current amplitudes were determined by manual fitting of appropriate functions to the corresponding histograms using the program Mac-Tac (Version 2.0, Instrutech).

For synchronization of electrical recordings with image acquisition, a trigger pulse was sent simultaneously to the electrical and optical setups.

Optical setup and data analysis

Apparatus, data acquisition, and automatic data analysis system were used as described in detail (Schmidt et al., 1996). In brief, samples were illuminated for 6 ms by 528 nm light from an argon ion laser (Innova 306, Coherent) using a 60× objective (Olympus, NA = 1.2) in an epifluorescence microscope (Axiovert 135TV, Zeiss). The laser beam was defocused to an area of 1400 μm^2 at a mean intensity of 1.4kW/cm^2. Excitation light was effectively blocked by appropriate filter combinations (custom-made TRITC/Cy5 dichroic and emission filter, Omega; OG550, Schott). Cy3 and Cy5 emission were split by placing a custom dichroic wedge (1° beam separation, Chroma) into the parallel optical path (Cognet et al., 2000). Both images were obtained by a liquid-nitrogen cooled slow-scan CCD-camera system (MicroMax 1300-PB, Roper Scientific) and stored on a PC. The samples were consecutively observed, with the delay between two observations set at 7, 10, 20, 100, or 200 ms. The signal of individual monomers and dimers was automatically analyzed by fitting a two-dimensional Gaussian profile, yielding the position with an accuracy of ~40nm. The quality of the wavelength separation was tested using a bilayer with gA-Cy3 only. No significant cross talk was observed. In addition, no direct excitation of pF-Phe-gA-Cy5 was found at 528nm excitation.

RESULTS

Design of recording apparatus

Apparatus designed to permit simultaneous optical and electrical recording of gA channels is shown diagrammatically in Fig. 1. Horizontal bilayers containing gramicidin molecules

with either a donor dye (Cy3) or an acceptor dye (Cy5) are imaged in the far field using a cooled CCD camera configured to record images in two channels—green emission from Cy3 and red emission from Cy5. The 528-nm line of an argon ion laser is used for excitation. Upon dimerization of a Cy3-peptide with a Cy5-peptide, the donor and acceptor dyes are ~50 Å apart, a distance that should lead to >50% FRET efficiency because the Förster radius for this donor-acceptor is 53 Å (Bastiaens and Jovin, 1998; Ha, 2001). Silver/silver chloride electrodes on each side of the membrane are connected to a patch-clamp amplifier that applies a voltage across the membrane and measures the current that results. Dimerization is detected electrically as a step increase in this current.

Due to the symmetric composition of both membrane leaflets, dimers of different types can form—Cy3/Cy3, Cy5/Cy5, and Cy3/Cy5. The latter heterodimer species can occur in two orientations with respect to the applied electrical field across the membrane. Only heterodimers are expected give an optical (FRET) signal whereas homodimers will not. To be able to distinguish heterodimers and homodimers electrically, we changed the N-terminal residue of gA-Cy5 to pF-Phe in place of valine. Koeppe, 2nd and Andersen have shown that ion flux is inhibited in pF-Phe-gA channels via unfavorable ion-dipole interactions compared to gA. As a result, gA/gA, pF-Phe-gA/gA, and pF-Phe-gA/pF-Phe-gA channels are easily distinguished by their conductances (Koeppe et al., 1990).

Synthesis and characterization of dye-labeled peptides

Modified gramicidin peptides were derivatized at their C-terminal ends to install the cyanine dyes Cy3 and Cy5 (Fig. 1 B). Added groups at the C-terminus of gramicidin have been found to be well tolerated and do not lead to aberrant folding of the peptide in the membrane (Lougheed et al., 2001). The ability of the peptides to undergo FRET when dimerized was tested by combining peptides in lipid vesicles at peptide/lipid ratios where dimers predominate over monomers and where channels are known to be active via flux assays (Lougheed et al., 2001). Fig. 2 shows the FRET signal observed when gA-Cy3 and pF-Phe-gA-Cy5 peptides are present in the same vesicles; as a control, a solution containing separate gA-Cy3 and pF-Phe-gA-Cy5 vesicle preparations was examined. When excited at 528 nm, little direct excitation of the acceptor is observed whereas sensitized emission via FRET is evident. Because of the presence of homodimers together with heterodimers in these vesicles, the apparent efficiency of FRET is diminished relative to a pure heterodimer case. A quantitative evaluation of the FRET efficiency is complicated by the complexity of vesicles geometry (Estep and Thompson, 1979; Fung and Stryer, 1978), however, a qualitative estimate of >50% FRET can be calculated by the method of Clegg (Clegg et al., 1992).
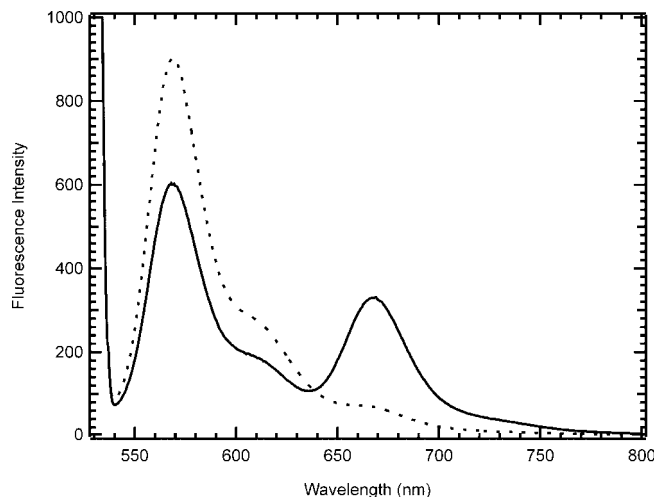

FIGURE 2 (*Dotted line*) Fluorescence emission spectrum of a solution containing 0.5 μM gA-Cy3 donor and 0.5 μM pF-Phe-gA-Cy5 acceptor peptides incorporated individually into separate unilamellar lipid vesicles. (*Solid line*) Fluorescence emission spectrum of 0.5 μM gA-Cy3 donor and 0.5 μM pF-Phe-gA-Cy5 acceptor peptides coincorporated into a single population of unilamellar lipid vesicles. Sensitized emission is evident. (Excitation at 520 nm, 10-nm excitation and emission slit widths, lipid concentration: 6.4 mM dioleoyl-phosphatidylcholine).

Single-channel electrical recordings were made with pure gA-Cy3 and with pure pF-Phe-gA-Cy5 with 1 M KCl as the electrolyte and an applied voltage of 100 mV. Single-channel current amplitude histograms are shown in Fig. 3. Single-channel conductances and lifetimes are collected in Table 1. The pF-Phe-gA-Cy5 channels exhibit ~60% of the conductance of pure gA-Cy3 channels similar to the difference observed between gA and pF-Phe-gA (Koeppe et al., 1990). The average lifetimes (τ) of each type of channel are ~1 s, similar to gA. The similarity in behavior between these dye-modified channels and native gramicidin in terms of their electrical characteristics argues that they form standard channels in membranes as expected for C-terminal derivatives of gA.

When both pF-Phe-gA-Cy5 and gA-Cy3 peptides are added to the membrane, three peaks are seen in the current amplitude histogram (Fig. 3 C) as expected. In addition to homodimer channels, heterodimers of pF-Phe-gA-Cy5/gA-Cy3 with intermediate conductance are observed. Thus, heterodimers can be distinguished from homodimers electrically. When looking for correlations between optical and electrical signals, FRET is expected to occur only with a current of 1.65–1.75 pA (at 100 mV). Larger or smaller currents are due to homodimers and should not produce a FRET signal.

Simultaneous optical and electrical single-channel experiments

Fig. 4 shows a series of images of a bilayer containing fluorescent gA-Cy3 peptide irradiated at 528 nm and imaged
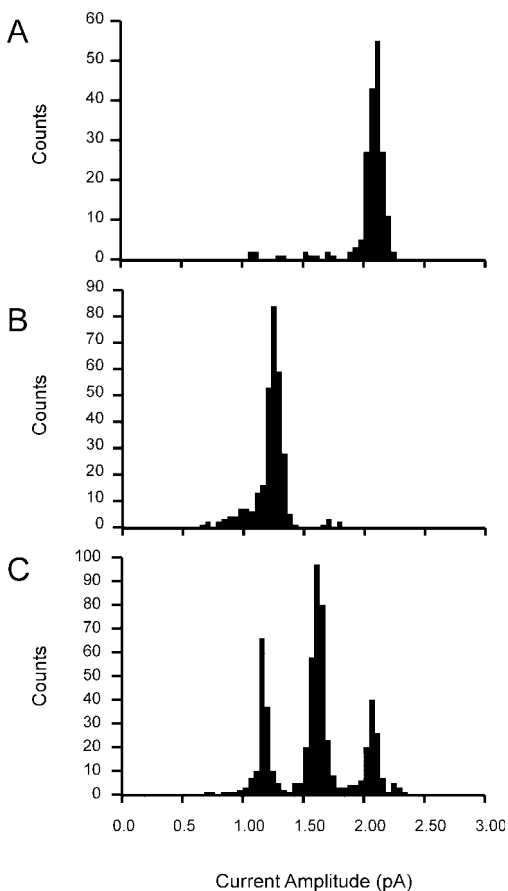
FIGURE 3 Single-channel current amplitude histograms for (*A*) gA-Cy3, (*B*) *p*F-Phe-gA-Cy5, and (*C*) a mixture of gA-Cy3 and *p*F-Phe-gA-Cy5 in diphytanoyl-phosphatidylcholine membranes (1 M KCl, 100 mV applied voltage). The peak at 1. 7 pA in (*C*) is due to heterodimer channels.

concentration of dimers was 0.05 channels/100 μm^2 (i.e., single gA-Cy3 homodimer channels were observed intermittently). Under these conditions, the total gA-Cy3 concentration can be estimated from the fluorescence image to be 15–30 molcules/100 μm^2 (or 2.5–5 $\times$ 10^{-17} mol/cm^2), as expected based on a peptide to lipid ratio of 1/10^7. The dimerization constant (K_A) is thus 1.3 $\times$ 10^{14} – 3.3 $\times$ 10^{13} cm^2/mol, close to that estimated from the multichannel data of Veatch and Stryer (Veatch et al., 1975).

Tracking the trajectories of individual gA-Cy3 molecules permits the estimation of monomer diffusion coefficients. A graph of mean square displacement versus time lag is shown in Fig. 6. From this, the monomer diffusion coefficient can be calculated to be 3.3 $\pm$ 0.1 μm^2 s^{-1} (3.3 $\times$ 10^{-8} cm^{2}s^{-1}). Some deviation from linearity at longer time lags was evident. This might reflect the fact that the bilayer area is small and bounded. There was no evidence for large-scale clustering of gramicidin molecules.

Dimer formation detected via single-pair FRET

The experimental arrangement permits imaging of Cy5 fluorescence simultaneously with Cy3 fluorescence during irradiation at 528 nm (Cy3 excitation). The bilayer shown in Fig. 5 contains only gA-Cy3 and is imaged in both channels. No fluorescence is detected in the Cy5 (*red*) channel demonstrating that Cy3 emission is effectively filtered. Likewise, no fluorescence was detected in the red channel when only *p*F-Phe-gA-Cy5 was present (data not shown), demonstrating that direct excitation of Cy5 with the 528-nm excitation beam was not significant.

When both peptides were present, bright dots were seen in the red channel (Fig. 7). As these fluorescent events were absent when only either peptide was added it is natural to ascribe those events to FRET signals caused gA-Cy3/*p*F-Phe-gA-Cy5 complexes. The events observed in the red channel were much less frequent than those in the green channel (Fig. 7), consistent with the fact that the green channel shows monomers and homodimers whereas the red channel should only show heterodimers. The large number of spots in the green channel prevented identification of which green spot a red spot corresponded to. Tracking the trajectories of several of the red spots permitted the estimation of a diffusion coefficient for the dimeric channel (Fig. 8). This was 3.0 $\pm$ 0.1 μm^2 s^{-1} (3.0 $\times$ 10^{-8} cm^{2}s^{-1}). This value is very similar to that reported by Tank et al., for a dansylated gramicidin C derivative in hydrated multi-bilayers of dimyristoyl-phosphatidylcholine using the fluo-

only in the green channel, which detects fluorescence from gA-Cy3 monomers and dimers. A bright ring is observed, as expected, for the torus of lipid and decane that supports the bilayer and forms the connection to the Teflon support. This torus is much thicker than the bilayer and contains most of the total peptide so it gives a bright signal. The bilayer appears black because it contains very few fluorophores. At the point indicated, a pulse of 5 V was applied to the membrane to rupture it. The transmembrane current increases abruptly because the bilayer resistance has been removed. A fluorescence image collected just after this event shows the torus has disappeared due to a massive rearrangement of lipid and decane.

Fig. 5 shows another bilayer containing gA-Cy3 where the peptide concentration was adjusted so that the time average

TABLE 1

Channel Type	*p*F-Phe-gA-Cy5 (homodimer) ($n = 209$)	gA-Cy3/*p*F-Phe-gA-Cy5 (heterodimers) ($n = 159$)	gA-Cy3 (homodimer) ($n = 138$)
Conductance*	12 $\pm$ 2 pS	17 $\pm$ 2 pS	21 $\pm$ 2 pS
Lifetime (s)	0.77	—	2.76

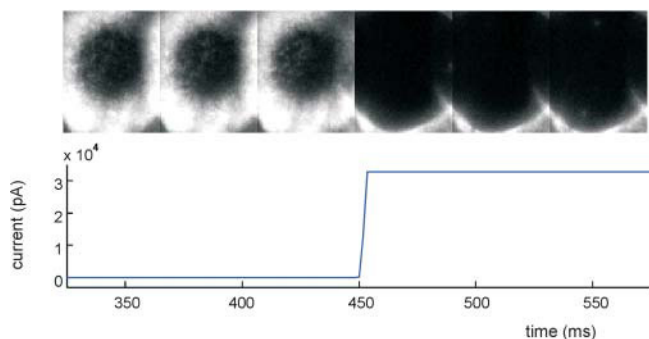*In 1 M KCl, diphytanoyl-phosphatidylcholine/decane membranes.

FIGURE 4   (*A*) Optical (fluorescence) image of a bilayer containing a low concentration of gA-Cy3. (*B*) Simultaneous electrical recording from the same membrane. At ~450 ms, a 5-V pulse was applied to break the membrane. The current increases abruptly and the subsequent image shows the massive rearrangement of the membrane and torus.

rescence recovery after photobleaching technique (Tank et al., 1982). The slightly enhanced mobility of the monomer compared to the dimer is consistent with previous measurements of the diffusion of single-leaflet-penetrating monomers and bilayer-spanning lipids (Nadler et al., 1985; Vaz et al., 1985).

To examine if there was a correlation between optical and electrical events, we made a series of experiments at peptide concentrations where only single-channel openings were observed. Fig. 9 shows examples of correlated events in which a bright dot appears in the red channel at the same time that a heterodimer channel (1.7–1.75 pA) is observed electrically. In Fig. 9 *A*, a heterodimer channel is observed that corresponds to a bright dot in the first two frames. The channel closes and the FRET signal disappears. Soon after, a gA-Cy3 homodimer channel is observed (2.1 pA) with no optical correlate, as expected. In Fig. 9 *B*, simultaneous optical and electrical events are observed for the last three frames of the image. A heterodimer channel opens briefly earlier in the recording but no optical correlate is observed.
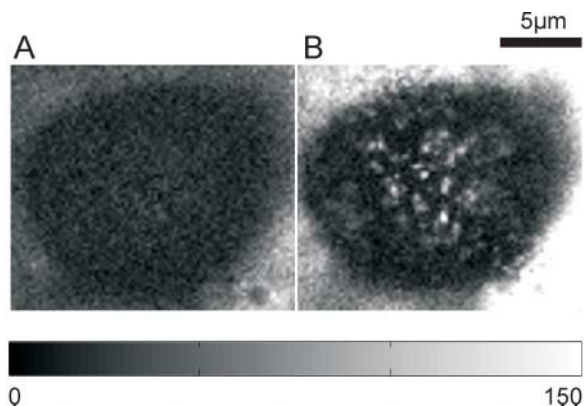

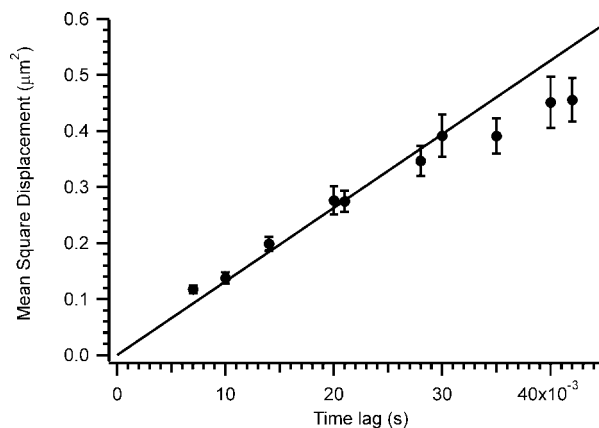FIGURE 5   Fluorescence images ((*A*) *red channel*, (*B*) *green channel*) of a membrane containing only gA-Cy3.

FIGURE 6   Diffusion of gA-Cy3 monomers. The mean square displacement, $\langle r^2(t_{lag}) \rangle = \langle (\vec{r}(t + t_{lag}) - \vec{r}(t))^2 \rangle$, of 222 trajectories was calculated for all time lags $t_{lag} = t_{ill} + t_{delay}$. The data show a linear increase with the time lag, as expected for free Brownian motion ($r^2 = 4Dt_{lag}$), with a diffusion constant, $D_m = 3.3 \pm 0.1 \ \mu m^2 \ s^{-1}$.

DISCUSSION

Design of the recording cell

The central aim of this study was to test the feasibility of combined optical and electrical recording measurements in a configuration that could prove applicable to the study of a wide range of ion channels. Several technical challenges had to be overcome to realize this goal. First, the membrane to be imaged must be within 100 μm of the glass coverslip because high numerical aperture objectives (with short working distances) are required to maximize collection of fluorescent photons. This requires that the aperture over which the membrane is painted must be formed in thin material (otherwise the vertical (*z*) position of the membrane is not well defined) that is suspended very close to the coverslip surface. If this material is not sufficiently rigid, it can simply sit on the glass coverslip, which leads to unstable membrane formation and poor electrical contact. Alternatively, it can become misshapen so that the painted bilayer is not parallel to the glass coverslip and the bilayer is not all in focus. We experimented with a number of different plastics as well as glass wafers. A functional system is shown in Fig. 1. The bilayer membrane was formed by painting a solution of lipid in decane across a small (40–70-μm diameter) hole in a thin (12 μm) Teflon film. Teflon-supported bilayers are widely used for single-channel electrical recording. Agarose and thicker pieces of Teflon surrounding the thin film provided some rigidity and facilitated bilayer formation while keeping the film within 100 μm of the coverslip. Chlorided silver foil provided the working electrode for the lower aqueous chamber. The entire cell together with the patch-clamp amplifier headstage was placed in a copper box that was in turn mounted on the microscope headstage. This provided excellent shielding from electrical noise. Further
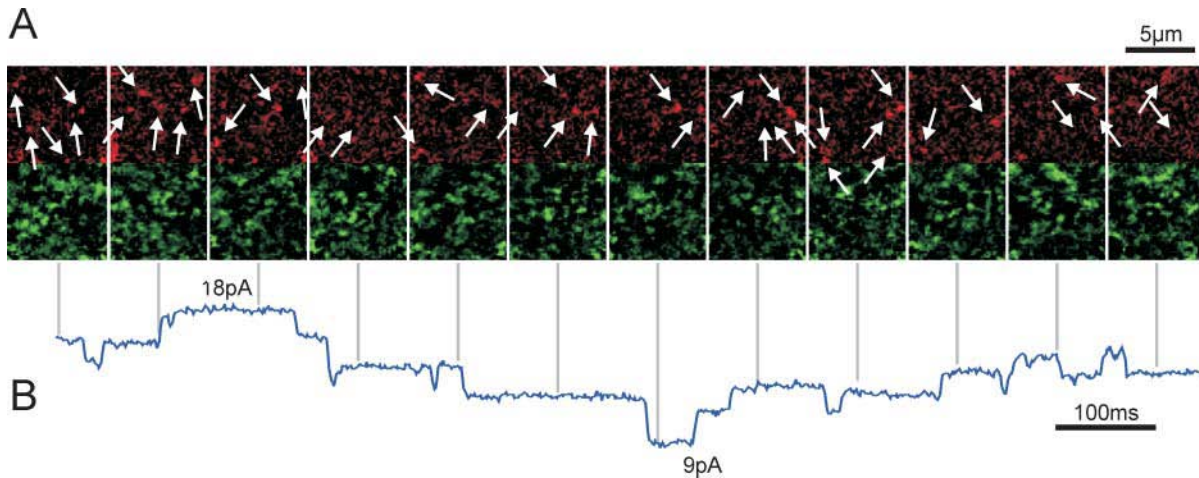
FIGURE 7 (*A*) Optical (fluorescence) images (*top: red channel, bottom: green channel*) of a bilayer containing sufficient gA-Cy3 and *p*F-Phe-gA-Cy5 to result in multiple simultaneous channel openings. FRET events (*bright dots in the red channel*) are indicated with arrows. For clarity, not all FRET events are indicated. (*B*) Simultaneous electrical recording from the same membrane. Vertical lines indicate the position of each image in the time record. The acquisition time for each image was 6 ms.

engineering might provide an improved design, however, as discussed more fully below.

Simultaneous optical and electrical recording: evidence for FRET

When donor and acceptor peptides were both present in the membrane, bright dots were seen in the acceptor emission channel consistent with the occurrence of FRET between donor and acceptor peptides. The probability that these FRET events originate from accidental proximity of donor and acceptor peptides diffusing laterally in the bilayer can be shown to be negligible as follows: Let us assume we have a planar membrane of area S in which molecules A and B can diffuse laterally with no specific attractive or repulsive interactions between molecules. The instantaneous probability of one (or more) B molecules being within a distance r of an A molecule is given by (Chandrasekhar, 1943):

$$p = 1 - \exp(-\pi r^2 S N_A [A][B]), \qquad (1)$$

where N_A is Avogadro's number and $[A]$ and $[B]$ are the surface concentrations of A and B respectively. If $[A] = [B] = 10^{-16}$ mol/cm^2, $r = 53$ Å (the Förster distance for Cy3/Cy5) and $S = 10^{-6}$ cm^2 (100 μm^2), then $p = 0.0032$ or ~0.3%.

The instantaneous probability for a FRET event occurring anywhere in the imaged area is thus small. If the molecules did not diffuse in the plane of the membrane (i.e., >53 Å or so) during the required time to obtain an image (~6 ms), then bright dots would be expected to be observed with this probability. However, from the diffusion measurements described above, monomers are indeed diffusing in the plane of the membrane with a diffusion coefficient of 3×10^{-8}

cm^{2}s^{-1}. The average time τ_D for a molecule to remain within a distance x of another molecule is given by:

$$\tau_D = \frac{x^2}{4D}. \qquad (2)$$

With $x = 53 \times 10^{-8}$ cm^2 and $D = 3 \times 10^{-8}$ cm^{2}s^{-1}, τ_D is 2.3 μs. Thus, for a bright dot to be observed, a series of random FRET events would have to occur during a significant fraction of the 6 ms imaging time, all within the area of a few pixels. Therefore it is highly unlikely that the bright dots observed in Figs. 7 and 9 are the result of adventitious associations of gA peptides.

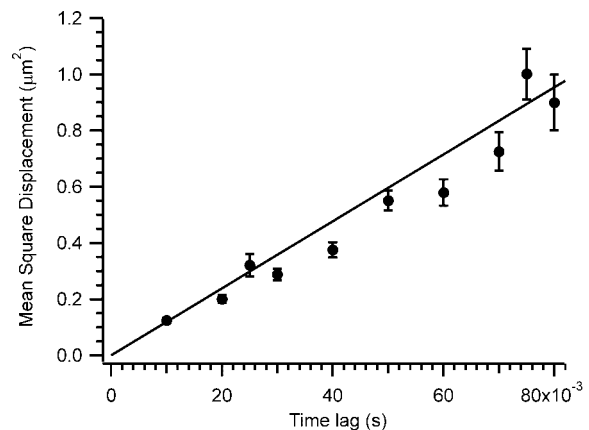Instead, the characteristics of these FRET events are exactly as predicted by the standard model of gramicidin

FIGURE 8 Diffusion of gA-Cy3/*p*F-Phe-gA-Cy5 dimers. The mean square displacement, $\langle r^2(t_{lag}) \rangle = \langle (\vec{r}(t + t_{lag}) - \vec{r}(t))^2 \rangle$, of 62 dimer trajectories was calculated for all time lags $t_{lag} = t_{ill} + t_{delay}$. The data show a linear increase with the time lag, as expected for free Brownian motion ($r^2 = 4Dt_{lag}$), with a diffusion constant, $D_d = 3.0 \pm 0.1$ μm^2 s^{-1}.
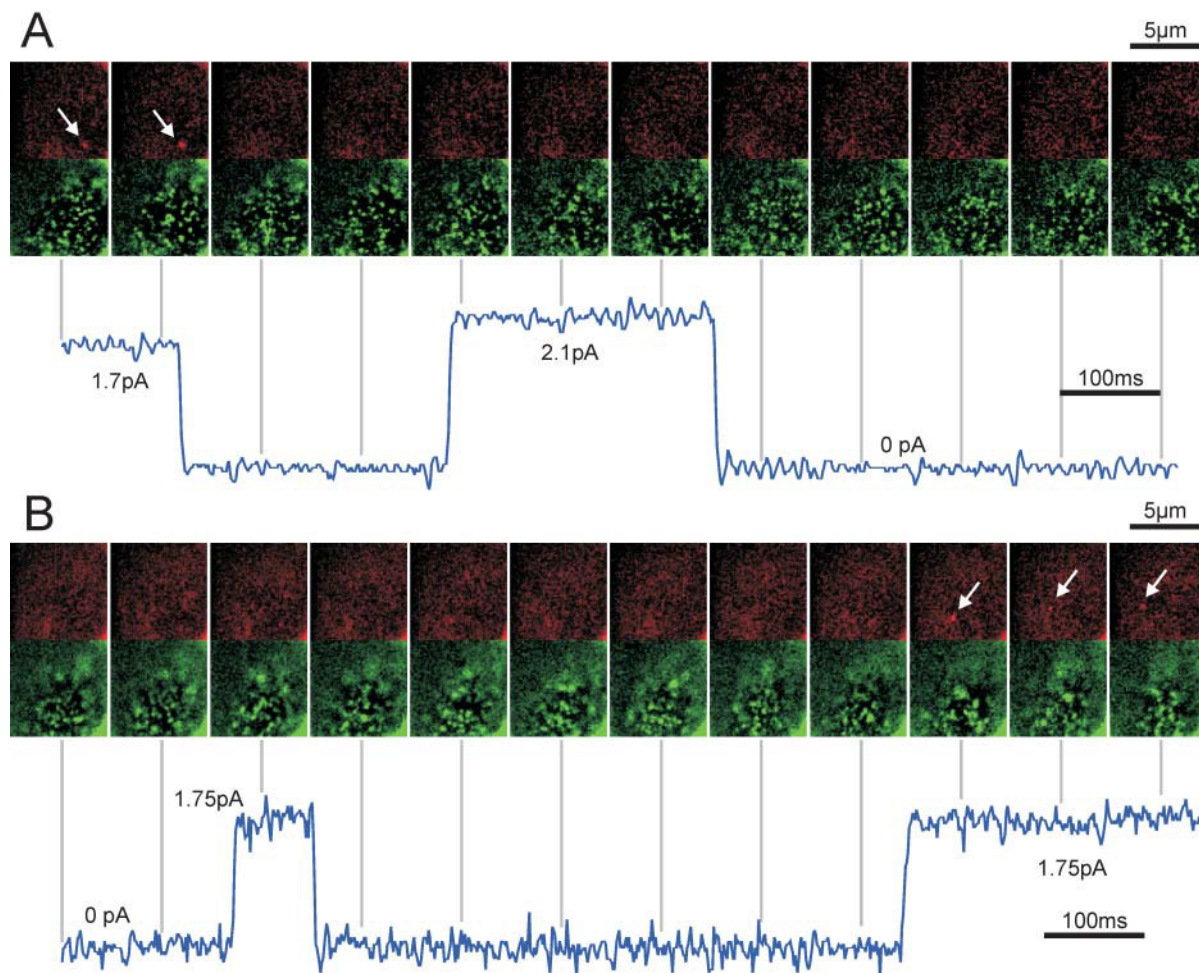
FIGURE 9   Optical (fluorescence) images (*top: red channel, bottom: green channel*) of two different bilayers (*A*, *B*) containing sufficient gA-Cy3 and *p*F-Phe-gA-Cy5 to result in single channel openings. FRET events (*bright dots in the red channel)* are indicated with arrows. Simultaneous electrical recording from the same membrane are shown below each row of images. Vertical lines indicate the position of each image in the time record. The acquisition time for each image was 6 ms. In (*A*), a heterodimer channel is observed that corresponds to a bright dot in the first two frames. The channel closes and the FRET signal disappears. In frames 5–7, a gA-Cy3 homodimer channel is observed (2.1 pA) with no optical correlate, as expected. In (*B*), simultaneous optical and electrical events are observed for the last three frames of the image. A heterodimer channel opens briefly earlier in the recording but no optical correlate is observed.

channel gating. The events have lifetimes on the order of 1 s, consistent with the open channel lifetime, their number compared to the number of fluorescent monomers is consistent with the expected dimerization constant for gramicidin peptides in these membranes, and they diffuse in the plane of the membrane with the expected diffusion coefficient for gramicidin dimers. All these observations support the conclusion that the observed events do correspond to gramicidin channel gating events.

Simultaneous optical and electrical recording: sources of uncorrelated events

In addition to the correlated electrical and optical events just described, uncorrelated signals were also observed. For instance, electrical signals were observed without an optical correlate. This may occur for a number of reasons.

First, a bleaching event or a dye photoisomerization event (Widengren and Schwille, 2000) may have occurred during previous illuminations leading to destruction of the donor or—less likely—the acceptor fluorophore without affecting the conductance properties of the channel. Because the dyes are some distance from the channel entrance, a change in the dye structure would not be expected to affect conductance significantly. Second, the channel may occur in some part of the membrane that is outside the imaging area, is out of focus, or is too near the torus to be reliably identified. Third, if the dyes are not freely rotating, certain donor acceptor orientations or distances may result in very inefficient FRET. Because the approximate distance between the centers of the conjugated chains of each dye is close to the Förster distance, relatively small increases in donor-acceptor separation could lead to substantial drops in FRET efficiency.

Interestingly, FRET signals were also observed even when no ion channels were detected electrically. This suggests that peptides can dimerize but may not always conduct ions. This might occur if a dimer formed in a nonbilayer part of the image. For instance, microlenses formed of lipid and decane are known to occur in painted bilayers under certain conditions (White, 1986; Tien, 1974). Another possible source of FRET events without electrical correlates could be the occurrence of double-stranded dimers with conductances too low to measure. A variety of double-stranded dimeric forms of gramicidin are known to occur in organic solvents (Woolley and Wallace, 1992). Although multichannel combined optical and electrical measurements are consistent with all dimers being conducting, the accuracy of the measurement is not high (Veatch et al., 1975) so that a subpopulation of nonconducting dimers might exist. A third possibility is that these represent some sort of intermediate on the path to channel formation. The presence of flickers (brief closing events in single-channel recordings) (Ring, 1986; Heinemann and Sigworth, 1991) suggests the presence of at least a short-lived nonconducting species that is closely related to a conducting dimer. A nonconducting dimeric intermediate has also been proposed to explain the kinetics of gramicidin channel formation after a voltage jump (Stark et al., 1986; Cifu et al., 1992; Stark, 1992). Single molecule optical imaging thus offers the possibility of detecting structural rearrangements of non-conducting states of ion channels.

Strategies for improvement

Currently, the cell design permits electrical measurements to be made easily and with sufficiently low noise (even in the presence of the numerous high power sources of the optical setup) to permit heterodimer channels to be recognized without difficulty. The electrical stability of the membranes is high and recording can be made for several hours from the same membrane. Although simultaneous single-channel optical and electrical recording can clearly be achieved as shown in Figs. 4, 5, 7, and 9, the ease of such measurements would be greatly improved if the strength of the FRET signal over background could be increased or the degree of background fluorescence fluctuation could be decreased. The noise levels in the optical measurements currently make automated image analysis problematic. A statistical analysis of the degree of correlation between optical and electrical signals therefore would be misleading at this stage. Currently the strength of the FRET signal is at most ~50% that of a directly excited fluorophore. This may be improved by having dyes closer together so that nearly complete FRET occurs upon peptide dimerization. Dyes with a longer Förster distance might be employed, although these would have to maintain the low cross talk and photobleaching levels of the Cy3 and Cy5 dyes to be useful.

Movements of the torus and the bilayer can alter the extent of background fluorescence from frame to frame. If the aperture supporting the bilayer were more rigid, these fluctuations might be reduced. Apertures formed in glass wafers (Fertig et al., 2001) or silicon (Pantoja et al., 2001) are attractive for their rigidity and may be better suited for these measurements than apertures in Teflon films. Moreover, if the Teflon disk becomes misshapen during membrane application, it is possible that the bilayer is not horizontal with respect to the microscope objective. Any part of the bilayer that is out of focus may contribute electrical signals that will not have optical correlates.

The use of other lipid solvents may reduce the size of the torus and its contribution to the total fluorescence signal (White, 1986). Altering the lipid and solvent composition of the membrane might also reduce the occurrence of micro-lenses, which may be a source of optical events without electrical correlates. In the gramicidin case, particularly, different lipid solvent compositions might be employed to increase the dimerization constant and thereby reduce the number of monomers required to see single dimers in membranes. This too should reduce the total fluorescence signal and make FRET events easier to recognize. However, channel lifetimes become many seconds long in such membranes (Elliott et al., 1983) so that gating events would be difficult to observe.

CONCLUSION

These experiments clearly demonstrate the feasibility of correlated electrical and optical measurements on single fluorescently labeled ion channels. The fact that the well-studied gramicidin A channel system behaves essentially as expected when imaged at the single molecule level provides confidence that this combined optical and electrical approach can be used to uncover gating mechanisms in a wide variety of ion channels.

REFERENCES

Anzai, K., K. Ogawa, T. Ozawa, and H. Yamamoto. 2001. Quantitative comparison of two types of planar lipid bilayers—folded and painted—with respect to fusion with vesicles. *J. Biochem. Biophys. Methods.* 48:283–291.

Arseniev, A. S., I. L. Barsukov, V. F. Bystrov, A. L. Lomize, and A. Ovchinnikov Yu. 1985. 1H-NMR study of gramicidin A transmembrane ion channel. Head-to-head right-handed, single-stranded helices. *FEBS Lett.* 186:168–174.

Bamberg, E., and P. Lauger. 1973. Channel formation kinetics of gramicidin A in lipid bilayer membranes. *J. Membr. Biol.* 11:177–194.

Bastiaens, P. I. H., and T. M. Jovin. 1998. Fluorescence resonance energy transfer microscopy. *In* Cell Biology: A Laboratory Handbook. 2nd ed., vol. 3. J. E. Celis, editor. Academic Press, New York. 136–146.

Cha, A., G. E. Snyder, P. R. Selvin, and F. Bezanilla. 1999. Atomic scale movement of the voltage-sensing region in a potassium channel measured via spectroscopy. *Nature.* 402:809–813.

Chandrasekhar, S. 1943. Stochastic problems in physics and astronomy. *Rev. Mod. Phys.* 15:1–89.

Cifu, A. S., R. E. Koeppe 2nd, and O. S. Andersen. 1992. On the supramolecular organization of gramicidin channels. The elementary conducting unit is a dimer. *Biophys. J.* 61:189–203.

Clegg, R. M., A. I. Murchie, A. Zechel, C. Carlberg, S. Diekmann, and D. M. Lilley. 1992. Fluorescence resonance energy transfer analysis of the structure of the four-way DNA junction. *Biochemistry.* 31:4846–4856.

Cognet, L., G. S. Harms, G. A. Blab, P H. M. Lommerse, and T. Schmidt. 2000. Simultaneous dual-color and dual-polarization imaging of single molecules. *Appl. Phys. Lett.* 77:4052–4054.

Elliott, J. R., D. Needham, J. P. Dilger, and D. A. Haydon. 1983. The effects of bilayer thickness and tension on gramicidin single-channel lifetime. *Biochim. Biophys. Acta.* 735:95–103.

Estep, T. N., and T. E. Thompson. 1979. Energy transfer in lipid bilayers. *Biophys. J.* 26:195–207.

Fertig, N., C. Meyer, R. H. Blick, C. Trautmann, and J. C. Behrends. 2001. Microstructured glass chip for ion-channel electrophysiology. *Phys. Rev. E.* 64:040901–040904.

Fung, B. K., and L. Stryer. 1978. Surface density determination in membranes by fluorescence energy transfer. *Biochemistry.* 17:5241–5248.

Glauner, K. S., L. M. Mannuzzu, C. S. Gandhi, and E. Y. Isacoff. 1999. Spectroscopic mapping of voltage sensor movement in the Shaker potassium channel. *Nature.* 402:813–817.

Goulian, M., O. N. Mesquita, D. K. Fygenson, C. Nielsen, O. S. Andersen, and A. Libchaber. 1998. Gramicidin channel kinetics under tension. *Biophys. J.* 74:328–337.

Greathouse, D. V., R. E. Koeppe 2nd, L. L. Providence, S. Shobana, and O. S. Andersen. 1999. Design and characterization of gramicidin channels. *Methods Enzymol.* 294:525–550.

Ha, T. 2001. Single-molecule fluorescence resonance energy transfer. *Methods.* 25:78–86.

Harms, G. S., L. Cognet, P. H. Lommerse, G. A. Blab, H. Kahr, R. Gamsjager, H. P. Spaink, N. M. Soldatov, C. Romanin, and T. Schmidt. 2001. Single-molecule imaging of L-type Ca^{2+} channels in live cells. *Biophys. J.* 81:2639–2646.

Heinemann, S. H., and F. J. Sigworth. 1991. Open channel noise. VI. Analysis of amplitude histograms to determine rapid kinetic parameters. *Biophys. J.* 60:577–587.

Helluin, O., J. Y. Dugast, G. Molle, A. R. Mackie, S. Ladha, and H. Duclohier. 1997. Lateral diffusion and conductance properties of a fluorescein-labelled alamethicin in planar lipid bilayers. *Biochim. Biophys. Acta.* 1330:284–292.

Hladky, S. B., and D. A. Haydon. 1970. Discreteness of conductance change in bimolecular lipid membranes in the presence of certain antibiotics. *Nature.* 5231:451–453.

Ide, T., and T. Yanagida. 1999. An artificial lipid bilayer formed on an agarose-coated glass for simultaneous electrical and optical measurement of single ion channels. *Biochem. Biophys. Res. Commun.* 265:595–599.

Ishii, Y., and T. Yanagida. 2000. Single molecule detection in life sciences. *Single Mol.* 1:5–16.

Ketchem, R. R., W. Hu, and T. A. Cross. 1993. High-resolution conformation of gramicidin A in a lipid bilayer by solid-state NMR. *Science.* 261:1457–1460.

Koeppe 2nd, R. E., and O. S. Anderson. 1996. Engineering the gramicidin channel. *Annu. Rev. Biophys. Biomol. Struct.* 25:231–258.

Koeppe 2nd, R. E., J. L. Mazet, and O. S. Andersen. 1990. Distinction between dipolar and inductive effects in modulating the conductance of gramicidin channels. *Biochemistry.* 29:512–520.

Koeppe 2nd, R. E., J. A. Paczkowski, and W. L. Whaley. 1985. Gramicidin K, a new linear channel-forming gramicidin from Bacillus brevis. *Biochemistry.* 24:2822–2826.

Lougheed, T., V. Borisenko, C. E. Hand, and G. A. Woolley. 2001. Fluorescent gramicidin derivatives for single-molecule fluorescence and ion channel measurements. *Bioconjug. Chem.* 12:594–602.

MacDonald, A. G., and P. C. Wraight. 1995. Combined spectroscopic and electrical recording techniques in membrane research: prospects for single channel studies. *Prog. Biophys. Mol. Biol.* 63:1–29.

Maduke, M., C. Miller, and J. A. Mindell. 2000. A decade of CLC chloride channels: structure, mechanism, and many unsettled questions. *Annu. Rev. Biophys. Biomol. Struct.* 29:411–438.

Nadler, W., P. Tavan, and K. Schulten. 1985. A model for the lateral diffusion of "stiff" chains in a lipid bilayer. *Eur. Biophys. J.* 12:25–31.

Pantoja, R., D. Sigg, R. Blunck, F. Bezanilla, and J. R. Heath. 2001. Bilayer reconstitution of voltage-dependent ion channels using a microfabricated silicon chip. *Biophys. J.* 81:2389–2394.

Ring, A. 1986. Brief closures of gramicidin A channels in lipid bilayer membranes. *Biochim. Biophys. Acta.* 856:646–653.

Sakmann, B., and E. Neher. 1984. Patch clamp techniques for studying ionic channels in excitable membranes. *Annu. Rev. Physiol.* 46:455–472.

Sarges, R., and B. Witkop. 1965. Gramicidin A V. The structure of valine- and isoleucine-gramicidin A. *J. Am. Chem. Soc.* 87:2011–2020.

Schmidt, T., G. J. Schütz, W. Baumgartner, H. J. Gruber, and H. Schindler. 1996. Imaging of single molecule diffusion. *Proc. Natl. Acad. Sci. USA.* 93:2926–2929.

Schütz, G. J., V. P. Pastushenko, H. J. Gruber, H. G. Knaus, B. Pragl, and H. Schindler. 2000a. 3D imaging of individual ion channels in live cells at 40nm resolution. *Single Mol.* 1:25–31.

Schütz, G. J., M. Sonnleitner, P. Hinterdorfer, and H. Schindler. 2000b. Single molecule microscopy of biomembranes (review). *Mol. Membr. Biol.* 17:17–29.

Selig, J. 1981. Physical properties of model membranes and biological membranes. *In* Membranes and Intercellular Communication. R. Balian, M. Chabre, and P. F. Devaux, editors. North Holland, Amsterdam. 16–78.

Sigworth, F. J. 1994. Voltage gating of ion channels. *Q. Rev. Biophys.* 27:1–40.

Sonnleitner, A., G. J. Schutz, and T. Schmidt. 1999. Free Brownian motion of individual lipid molecules in biomembranes. *Biophys. J.* 77:2638–2642.

Stark, G. 1992. Arguments in favor of an aggregational model of the gramicidin channel: a reply. *Biophys. J.* 61:588–589.

Stark, G., M. Strassle, and Z. Takacz. 1986. Temperature-jump and voltage-jump experiments at planar lipid membranes support an aggregational (micellar) model of the gramicidin A ion channel. *J. Membr. Biol.* 89:23–37.

Tank, D. W., E. S. Wu, P. R. Meers, and W. W. Webb. 1982. Lateral diffusion of gramicidin C in phospholipid multibilayers. Effects of cholesterol and high gramicidin concentration. *Biophys. J.* 40:129–135.

Tien, H. T. 1974. Bilayer Lipid Membranes (BLM): Theory and Practice. M. Dekker, New York.

Vaz, W., D. Hallmann, R. Clegg, A. Gambacorta, and M. De Rosa. 1985. A comparison of the translational diffusion of a normal and a membrane-spanning lipid in L alpha phase 1-palmitoyl-2-oleoylphosphatidylcholine bilayers. *Eur. J. Biophys.* 12:19–24.

Veatch, W. R., R. Mathies, M. Eisenberg, and L. Stryer. 1975. Simultaneous fluorescence and conductance studies of planar bilayer membranes containing a highly active and fluorescent analog of gramicidin A. *J. Mol. Biol.* 99:75–92.

Weiss, L. B., and R. E. Koeppe 2nd. 1985. Semisynthesis of linear gramicidins using diphenyl phosphorazidate (DPPA). *Int. J. Pept. Protein Res.* 26:305–310.

White, S. 1986. The physical nature of planar bilayer membranes. *In* Ion Channel Reconstitution. C. Miller, editor. Plenum, New York. 3–35.

Widengren, J., and P. Schwille. 2000. Characterization of photoinduced isomerization and back-isomerization of the cyanine dye Cy5 by fluorescence correlation spectroscopy. *J. Phys. Chem. A.* 104:6416–6428.

Woolley, G. A., and B. A. Wallace. 1992. Model ion channels: gramicidin and alamethicin. *J. Membr. Biol.* 129:109–136.